International Journal of Microwave and Wireless Technologies, 2017, 9(8), 1687–1693.
doi:10.1017/S1759078717000289

RESEARCH PAPER

Fractional Fourier transform-based chirp radars for countering self-protection frequency-shifting jammers

SAMER BAHER SAFA HANBALI AND RADWAN KASTANTIN

Self-protection deceptive jammers create at the radar receiver output multiple-false targets that are impossible to isolate in both time and frequency domains. In this paper, we introduce a novel technique based on fractional Fourier transform (FrFT) to discriminate between the true target echo and those false targets in the case of frequency-shifting jammers. In fact, we exploit the capability of the FrFT to resolve, in a matched manner, spectra that are overlapping in time and frequency. This is a property that cannot be achieved using a standard matched filter. The theoretical analysis of this technique is presented and its effectiveness is verified by simulation.

Keywords: Chirp radars, Frequency-shifting jamming, Anti-jamming technique, Fractional Fourier transform

Received 28 November 2016; Revised 2 March 2017; Accepted 5 March 2017; first published online 3 April 2017

I. INTRODUCTION

Chirp waveform is one of the most used signals in radars due to its high Doppler tolerance [1]. But chirp radars are vulnerable to different types of deceptive jammers such as digital radio frequency memory (DRFM) repeater jammers that have been widely used in electronic counter measures (ECM). Since DRFM jammers retransmit the jamming pulses behind the true target echo, they can be recognized by radar systems easily [2]. This can be overcome by instantaneously retransmitting the radar pulse after shifting it in frequency [3].

Frequency-shifting jammers benefit from the well-known range-Doppler coupling property of chirp waveform, where a copy of the radar signal shifted in frequency can be transmitted as an echo to the radar to confuse it, because the jammer signal in this case looks like the radar return [3].

Usually, matched filter detection is used in surveillance radars. Unfortunately, the optimum detection of chirp signals by a matched filter cannot distinguish the true target from the false one in the time domain, because they are interchangeable in time, i.e. the false target may come before or after the true one. Also in the frequency domain, their spectra may be overlapping, which make them impossible to isolate. In this paper, we use the fractional Fourier transform (FrFT) to overcome these problems because it compresses and resolves the overlapping true target echo and jamming pulses in a matched manner in the fractional domain.

Department of Communication Engineering, Higher Institute of Applied Sciences and Technology, Damascus, Syria
Corresponding author:
S.B.S. Hanbali
Email: Samer.Hanbali@hiast.edu.sy

Recently, FrFT has been used in radar and sonar processing. In [4], the FrFT is applied to airborne synthetic aperture radar (SAR), where it is used to compress echoes from slow moving targets. In [5], an FrFT-based receiver is presented for the efficient detection and separation of overlapping chirp acoustic signals in the time domain. In [6], a radar-matched filter is implemented for a chirp radar using FrFT. In [7], the FrFT is used for fast detection and sweep rate estimation of pulse compression radar signals. In [8] FrFT is used to enhance monopulse processing in track radar, when additional targets appear in the look direction beam.

The commonly used electronic counter-countermeasures (ECCM) techniques are effective against some types of deceptive jammers. The coherence check technique compares between the pulse rising time and the detected target (range position after matched filter) in order to discriminate the true target. Of course, this is applicable only at a certain signal-to-noise ratio (SNR) of the incoming jamming pulse [9]. The pulse-width discriminator technique measures the width of each received pulse before the matched filter, also this is applicable only at a certain SNR [9]. If the received pulse is not of approximately the same width as the transmitted pulse it is rejected. Pulse repetition interval (PRI) jitter technique identifies the false targets returns if the deception jammer uses a delay that is greater than a PRI period to generate false targets return [10], but this technique is inefficient in the case of instantaneously retransmitting the radar pulse after frequency-shifting. The frequency agility technique changes the radio frequency of radar to make it impossible to know what the radio frequency of the next pulse will be. But if the jammer has a digital instantaneous frequency measurement receiver (DIFM) that measures approximately the first 50 ns of a pulse, it can quickly set to that radio frequency,

because modern radars typically have pulses of several microseconds long [10]. Orthogonal waveforms technique transmits successive orthogonal waveforms that have low cross-correlation [11], and when the jammer pulse lags behind the true target pulse, it will not benefit from the pulse compression gain, a situation that is not applicable in the case of frequency-shifting jammer. However, these techniques have some drawbacks that make them unsuitable to counter frequency-shifting jammer. Recently, FrFT filtering is used for combating high-power manmade interference against radar, with the assumption that the target position in the radar return window is known [12]. More recently, the works in [13–15] focus on countering deceptive jamming based on DRFM only. Also we addressed countering some types of frequency-shift jammer for the first time using sweep bandwidth agility [16].

On the basis of the research mentioned above, the problem of countering the different types of self-protection frequency-shifting jammer at low SNR, which has not yet been considered, needs to be investigated. In this paper, we use the FrFT at the radar receiver to counter these types of deceptive jammers against surveillance radar. The FrFT compresses the received signal in such a manner that the true target echo and the jamming signal are resolved so that they can be separated, each on its own. Then, after FrFT compression and separation, the resulting signals are returned to the frequency domain where their spectra can be compared with spectrum of the original radar chirp in terms of the center frequency and the bandwidth. Finally, the true target can be discriminated from the jamming ones.

The paper is organized as follows. Section II presents an overview of frequency-shifting jammers. In Section III, the chirp pulse compression using FrFT is given. In Section IV, the proposed radar anti-jamming technique is introduced. Finally, Matlab simulation results are demonstrated in Section V.

II. FREQUENCY-SHIFTING JAMMING

Repeater jammer can generate false target at the output of chirp radar detector by instantly shifting the frequency of radar signal, the amount of frequency shift determines the relative distances between false and true targets [3]. For self-protection jammer, the frequency-shifting generator is synchronized with the received radar signal therefore the true target and the jammer will have the same Doppler shift. Otherwise, the jammer frequency-shift will introduce an additional Doppler shift that is not correlated with the rate of range change of the false target, so the radar can discriminate against false targets [10]. The jammer retransmission may take different modes such as single false target jamming, multiple-false target jamming, and multiple-cover jamming [3].

A) Single false target jamming

Let $x(t)$ be the complex representation of the transmitted radar chirp [3]:

$$x(t) = \frac{1}{\sqrt{T}}\text{rect}\left(\frac{t}{T}\right)e^{j\mu\pi t^2}, \quad |t| < \frac{T}{2}, \tag{1}$$

where T is the chirp duration, $\mu = B/T$ is the frequency modulation slope, and B is the sweep bandwidth. Then, the complex representation of the jamming signal is given by [3]:

$$x_J(t) = x(t)e^{j2\pi f_J t} = e^{j2\pi f_J t + j\pi\mu t^2}, \quad |t| < \frac{T}{2}, \tag{2}$$

where f_J is the frequency shift of the jammer. The false target lags behind the true target when $f_J < 0$ and leads it when $f_J > 0$ by a distance of $d = cf_J/2\mu$.

B) Multiple-false targets jamming

In order to make it difficult for the radar to recognize the true target, several false targets could be generated simultaneously at the output of the matched filter. The frequency-shifting jammer divides radar pulse into N parts, and then modulates them by different frequencies. The first part is modulated by f_{J0}, and the modulated frequency of each part is [3]:

$$f_{Jn} = f_{J0} + (n-1)\Delta f_J, \quad n = 1, 2, 3, \ldots, N, \tag{3}$$

where Δf_J is the difference between the modulation frequencies of every two adjacent parts. The jamming signal now is [3]:

$$x_{Jn}(t) = e^{j2\pi f_{Jn}t + j\pi\mu t^2}, \quad t \in \left(-\frac{T}{2} + \frac{n-1}{N}T, -\frac{T}{2} + \frac{n}{N}T\right). \tag{4}$$

In this case, all the false target have the same amplitude, which is less than the amplitude of the true target by factor $1/N$.

C) Multiple-cover Jamming

The multiple-cover jamming is better than the single false target and multiple-false targets jamming [3], because it has an effect of blanket jamming. In this case, the jammer divides radar pulse into N parts at first, and then frequency modulate each part linearly. This gives false targets each of which covers some range in the frequency domain that is more efficient in jamming. The jamming signal is written now as [3]:

$$x_{Jn}(t) = e^{j2\pi f_{Jn}t + j\pi(\mu+\mu_J)t^2}, \quad t \in \left(-\frac{T}{2} + \frac{n-1}{N}T, -\frac{T}{2} + \frac{n}{N}T\right), \tag{5}$$

where μ_J is the frequency modulation slope of the jamming signal.

III. CHIRP PULSE COMPRESSION USING FRFT

The FrFT is a general form of the Fourier transform that transforms a function into an intermediate domain between time and frequency by rotating the time–frequency plane [17, 18]. Compared with Fourier transform as shown in Fig. 1(a), the FrFT of optimal angle, α_{opt}, applied to LFM

https://doi.org/10.1017/S1759078717000289 Published online by Cambridge University Press

(linear frequency modulated) signal, maximally concentrates the energy distribution of the signal in the fractional domain as shown in Fig. 1(b). This illustrates the use of the FrFT for pulse compression of chirp signals [19, 20].where u and v are the axes of the fractional domain, and α is the transform angle. Consider the axis rotation with angle α from (t, ω) to (u, v), as shown in Fig. 1(b). Then [21]:

$$u = t\cos\alpha + \omega\sin\alpha, \tag{6}$$

$$v = -t\sin\alpha + \omega\cos\alpha. \tag{7}$$

In this section, the mathematical analysis of the chirp pulse compression using FrFT is derived as follows.

The continuous FrFT of a signal $x(t)$ is given by [21, 22]:

$$X_\alpha(u) = \int_{-\infty}^{\infty} x(t)K_\alpha(t, u)dt, \tag{8}$$

where $K_\alpha(t, u)$ is the transform kernel and is given by [21, 22]:

$$K_\alpha(t,u) = \begin{cases} \sqrt{1-j\cot\alpha}\, e^{j2\pi(t^2+u^2/2)\cot\alpha - j2\pi ut\csc(\alpha)}, & \alpha \neq n\pi, n\in\mathbb{N} \\ \delta(t-u), & \alpha = 2n\pi, n\in\mathbb{N} \\ \delta(t+u), & \alpha = (2n+1)\pi, n\in\mathbb{N} \\ e^{-j2\pi tu}, & \alpha = (\pi/2)n, n\in\mathbb{N} \end{cases} \tag{9}$$

α being the transform fraction, and the inverses continuous FrFT is given by [21, 22]:

$$x(t) = \int_{-\infty}^{\infty} X_\alpha(u)K_{-\alpha}(u, t)du\ . \tag{10}$$

If F_α denote the operator corresponding to the FrFT of angle α, then the following properties hold [21, 22]:

- $F_0 = I$: zero rotation gives the same input.
- $F_{\pi/2} = F$: rotation by $\pi/2$ gives Fourier transform.
- $F_\alpha(F_\beta) = F_{\alpha+\beta}$: successive rotations are additive. This means: $F_\alpha(F_{-\alpha}) = F_0 = I$.

Applying the FrFT to the chirp signal given by equation (1) gives:

$$X_\alpha(u) = \sqrt{1-j\cot\alpha}\, e^{j\pi u^2\cot\alpha}\int_{-T/2}^{+T/2} e^{j\pi t^2(\mu+\cot\alpha) - j2\pi ut\csc(\alpha)}dt. \tag{11}$$

For arbitrary values of α, the integral in this equation involves an error function erf, which is a non-elementary function. But when:

$$\mu + \cot\alpha = 0. \tag{12}$$

A condition considered in [19, 20] as being optimal and denoted by α_{opt}, then equation (11) reduces to the simple sinc function:

$$X_{\alpha_{opt}}(u) = \sqrt{1-j\cot\alpha_{opt}}\, e^{j\pi u^2\cot\alpha_{opt}}.T\frac{\sin[\pi(u\csc\alpha_{opt})T]}{\pi(u\csc\alpha_{opt})T}. \tag{13}$$

Usually, $\mu \gg 1$, so equation (12) gives $\csc\alpha_{opt} \approx \mu$, and consequently, $\left|\sqrt{1-j\cot\alpha_{opt}}\right| \approx \sqrt{\mu}$. Hence,

$$\left|X_{\alpha_{opt}}(u)\right| = \sqrt{BT}\,.\frac{\sin(\pi Bu)}{\pi Bu}. \tag{14}$$

This is the same equation as that of the matched filter for a chirp signal when $BT \gg 1$. This means that the FrFT behaves like a matched filter for the chirp signal, therefore the traditional radar processing e.g. clutter rejection (Doppler filtering, Moving Target Indicator) [23], and constant false alarm rate (CFAR) can be used with FrFT. In addition, FrFT can separate the overlapping true target echo and jamming pulses which matched filter cannot do. However, the *SNR* at the output of the FrFT is half that at the output of the corresponding matched filter [24]:

$$SNR_{out,\ FrFT} = \frac{SNR_{out,\ matched\ filter}}{2}. \tag{15}$$

The computation complexity of the proposed technique depends on the implementation of FrFT. The fast FrFT is approximated using algorithms based on the fast Fourier transform (FFT) [17, 18], and it was shown that the fast FrFT has a computational complexity $O(N\ \log N)$ [25], which is suitable for practical application [5].

IV. THE PROPOSED RADAR ANTI-JAMMING TECHNIQUE

The properties of the retransmitted jamming pulse of each jammer that is presented in Section II are summarized in Table 1:

As shown in Table 1, the bandwidths of the retransmitted jamming pulses are narrower, or frequency shifted, in comparison with the transmitted radar pulse. However, they are overlapping with the true target echo in the time and frequency domains, and therefore, the matched filter cannot separate them. Here, the FrFT can be used to separate these overlapping pluses in a matched manner. After separation, they can be isolated and returned to frequency domain.

Figure 2 shows the block diagram of the proposed anti-jamming technique to counter frequency-shifting jammer using FrFT. The white boxes represent the conventional radar, and the grey boxes are added to implement the proposed technique. In the normal operating mode, the detection decision is taken from output (1), and when the radar needs to counter frequency-shifting jamming, the detection decision is taken from output (2).

As shown in Fig. 2, $r(t)$ is the baseband received signal, and $r(t)$ is the received signal after FrFT compression. $r(t)$ is composed of the sum of the true target echo $x(t)$, the jamming signal $x_J(t)$, and a white Gaussian noise $n(t)$.

Let f_J denotes the jammer's frequency shift. When the jammer shifts radar pulse by f_J (mode a), the received signal

https://doi.org/10.1017/S1759078717000289 Published online by Cambridge University Press

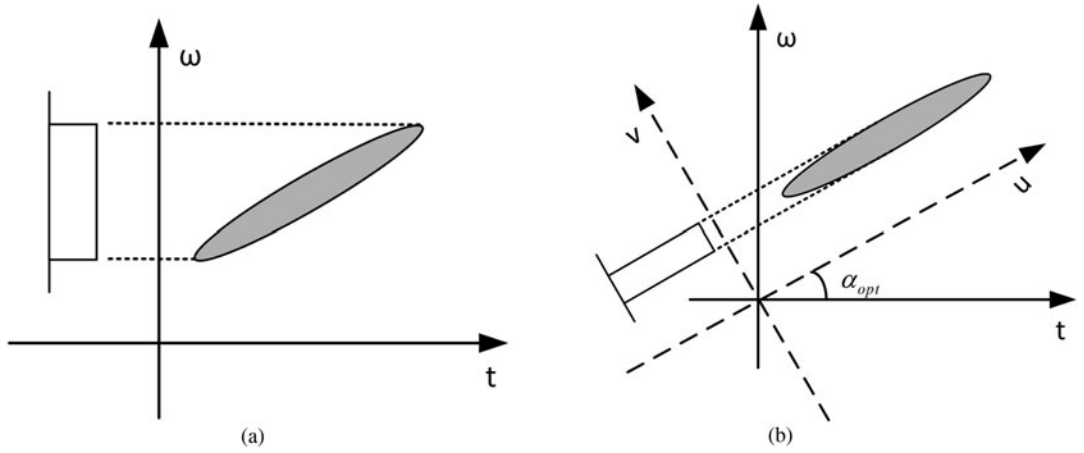

Fig. 1. (a) Projection of chirp signal onto Fourier domain (b) Projection of chirp signal onto fractional Fourier domain.

equals:

$$r(t) = x(t) + x_J(t) + n(t) = x(t) + x(t)e^{jw_J t} + n(t), \quad (16)$$

where $w_J = 2\pi f_J$.

The proposed technique is intended to compress both the true target and the jamming signals as follows.

$$F_\alpha(r(t)) = X_\alpha(u) + X_{J,\alpha}(u) + N_\alpha(u). \quad (17)$$

By using the modulation property of the FrFT [21, 22]:

$$F_\alpha(x(t)e^{jwt}) = e^{-jw^2(\sin\alpha\cos\alpha)/2 + juw\cos\alpha} X_\alpha(u - w\sin\alpha) \quad (18)$$

And at the optimum value of α, $X_\alpha(u)$ is given by equation (13), and using equations (2) and (12) we get:

$$F_{\alpha_{opt}}(r(t)) = \sqrt{1 - j\cot\alpha_{opt}}.T\left\{e^{j\pi u^2\cot\alpha_{opt}}\frac{\sin(\pi Bu)}{\pi Bu} + ke^{j\pi(u - w_J\sin\alpha_{opt})^2\cot\alpha_{opt}}\frac{\sin[\pi B(u - w_J\sin\alpha_{opt})]}{\pi B(u - w_J\sin\alpha_{opt})}\right\} + N_\alpha(u). \quad (19)$$

where $k = e^{-jw_J^2(\sin\alpha_{opt}\cos\alpha_{opt})/2 + juw_J\cos\alpha_{opt}}$.

Equation (19) shows that, apart from the noise component $N_\alpha(u)$, the output of the FrFT is composed of two sinc functions separated on the u-axis by a value of $w_J\sin\alpha_{opt}$. But:

$$w_J\sin\alpha_{opt} = \frac{2\pi f_J}{\mu}, \quad (20)$$

where $w_J = 2\pi f_J$ and $\sin\alpha_{opt} \approx 1/\mu$ as shown above.

As far as the noise is concerned, the FrFT is a linear transform, and therefore the probability distribution of the noise at its output does not change.

When the jammer divides radar pulse into N parts as shown in Table 1 (modes b and c), and modulates them by different frequencies, then there are N compressed jamming signals at the FrFT output, hence equation (19) becomes:

$$F_{\alpha_{opt}}(r(t)) = \sqrt{1 - j\cot\alpha_{opt}}.T\left\{e^{j\pi u^2\cot\alpha_{opt}}\frac{\sin(\pi Bu)}{\pi Bu} + \sum_{n=1}^{N}\frac{k_n e^{j\pi(u - w_{Jn}\sin\alpha_{opt})^2\cot\alpha_{opt}}}{N} \cdot \frac{\sin[\pi(B/N)(u - w_{Jn}\sin\alpha_{opt})]}{\pi(B/N)(u - w_{Jn}\sin\alpha_{opt})}\right\} + N_\alpha(u), \quad (21)$$

where $w_{Jn} = 2\pi f_{Jn}$, $k_n = e^{-jw_{Jn}^2(\sin\alpha_{opt}\cos\alpha_{opt})/2 + juw_{Jn}\cos\alpha_{opt}}$. As shown in equations (19) and (21), the main advantage of using FrFT instead of radar matched filter is its capability to separate the overlapping true target echo and jamming pulses.

In practice, all the signals received by radar, being true target return or false targets signals, are subject to Doppler shift, since the target is moving. The output of the FrFT includes the effect of that Doppler shift and must be compensated for when returning that output to the frequency domain. In the case of single false target (mode a), the Doppler compensation is required. It is not required in the case of multiple-false targets or multiple cover targets (modes b and c) because the jamming pulses have narrower bandwidth than the target pulse, thus they can be discriminated easily. The value of the Doppler shift is already estimated by the radar as shown in Fig. 2.

The process of the proposed technique is shown in Fig. 2, and it goes as follows:

Table 1. The properties of different jamming signals.

Mode	Repeater jammer type	The bandwidth of each jamming pulse	Spectrum offset of each jamming pulse
a	Frequency-shifting jamming, single false target	B	f_J
b	Frequency-shifting jamming, multiple-false targets	B/N	f_{Jn}
c	Frequency-shifting jamming, multiple-cover targets	B/N	f_{Jn}

https://doi.org/10.1017/S1759078717000289 Published online by Cambridge University Press

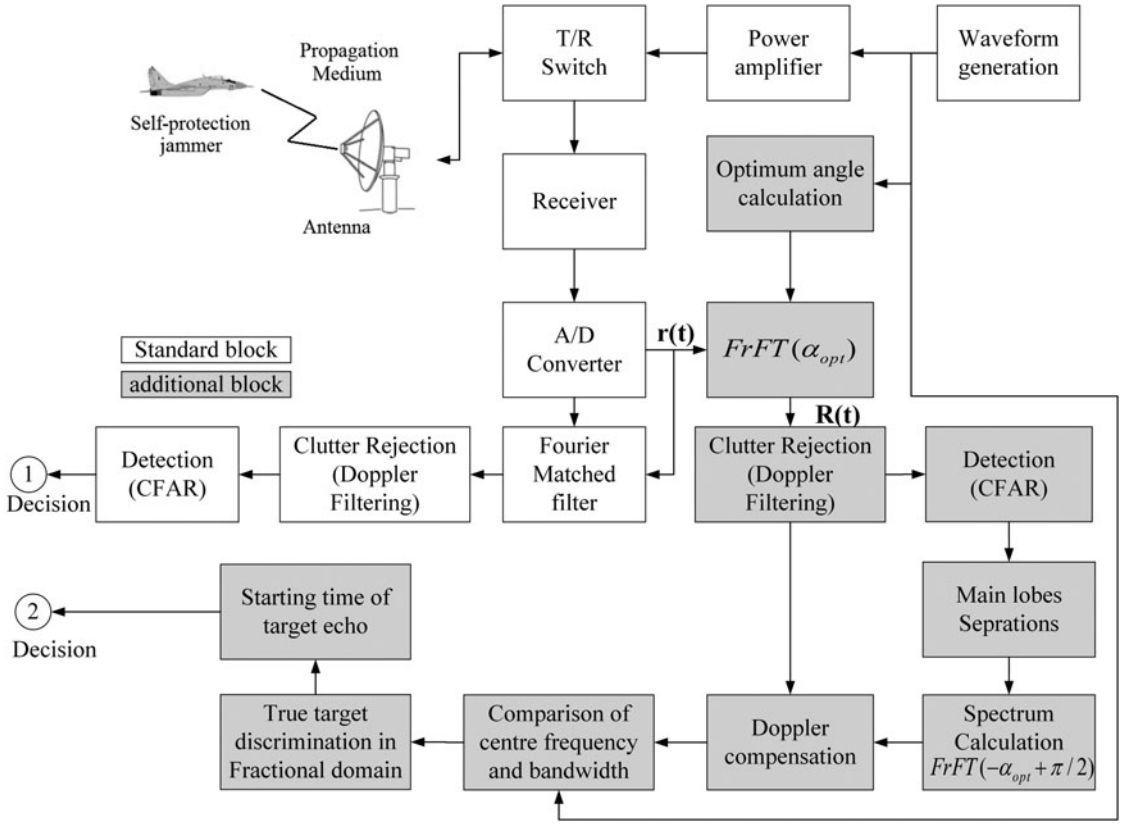

Fig. 2. The block diagram of the proposed radar anti-jamming technique. Non-shaded boxes represent the traditional radar structure, and the shaded ones represent the new part that exploit FrFT in the spectra resolution.

1. Calculate the optimum transform fraction α_{opt} of the FrFT in the discrete domain using equation (22) [5, 6].

$$\alpha_{opt} = -\tan^{-1}\left(\frac{F_s^2}{\mu L}\right), \tag{22}$$

where L is the number of samples in the time received window, and F_s is the sampling frequency used in the radar system. It is worth mentioning that α_{opt} is constant and known beforehand to the radar because it depends on the frequency modulation slope of the transmitted chirp.
2. The received signal (target echo and jamming signal) is compressed into Sinc function pulses using FrFT at α_{opt} that has a pulse compression gain of BT according to equation (14).
3. The Sinc pulses are isolated into independent signals after detection using CFAR. According to equation (14), it was shown that the FrFT behaves like a matched filter, the Rayleigh resolution equals −4 dB width of the main lobe [26]. Now, for each main lobe, the peak position sample and the adjacent samples (at the −4 dB level on both sides) are kept and the remaining samples are put to zero. In this manner, the different signals are individually separated, and then returned to the frequency domain by FrFT using the complementary value of α_{opt}, i.e. $\pi/2 - \alpha_{opt}$.
4. The −3 dB bandwidth and the center frequency of each spectrum is determined, and compared with the spectrum of the transmitted chirp after compensation for the Doppler shift. The signal that has the smallest differences of the center frequency and sweep bandwidth is considered as the true target.
5. Finally, the start time of the true target echo t_{st}, in the time domain, is calculated using equation (23) [6]:

$$t_{st} = \left\{\sin(\alpha_{opt})\left[\frac{-(B/2)}{(F_s/L)} + \frac{B(L/M_T)}{2\times(F_s/L)}\right] - P_P\right\} / \cos(\alpha_{opt}), \tag{23}$$

where P_P is the peak position of the compressed pulse in the fractional domain, and M_T is the number of signal samples: $M_T = T \times F_s$.

In electronic warfare, the jammer system does not use high jammer-to-signal ratio (JSR). This is because high jamming power makes the jammer vulnerable to hostile ARM (anti-radiation missile) attack. Nonetheless, when high JSR is used, a mutual target masking occurs; the strong false target that falls within the CFAR reference window will bias the threshold. Consequently, the conventional CFAR masks the weaker of the two closely spaced targets. Therefore, a modified CFAR is used such as the smallest-of cell average CFAR (SOCA-CFAR), trimmed mean (TM) or censored (CS) CFAR, and order statistics (OS) CFAR, which are designed to suppress mutual target masking. But these methods exhibit additional complexity, higher computational cost, and a higher CFAR loss, in terms of SNR, above the conventional CFAR due to the use of lower number of cells instead of N [26, 27].

https://doi.org/10.1017/S1759078717000289 Published online by Cambridge University Press

V. SIMULATION AND RESULTS

Next, we will use the proposed radar anti-jamming technique mentioned in Section IV, in order to counter the jammers assumed in this paper. For example, we assume these parameters. $B = 4$ MHz, $T = 100\ \mu$s, $M_T = 4000$, $F_s = 16$ MHz, $L = 32,000$ samples. The optimum order of FrFT is $a_{opt} = -0.1257$ after calculation using equation (22). As shown in Table 1, the jamming retransmission may take different modes (a–c)

A) Countering Jamming mode a

In this case, there is one false target in addition to the echo of the true target. Now, since $f_J \ll$ B, the two spectra of the true and false targets will be overlapping and cannot be separated in the frequency domain. But at the output of the FrFT they are well separated and they can be easily isolated in two different signals, as shown in Figs 3(a) and 3(b), respectively. The resultant two isolated FrFT signals are now returned to the frequency domain to give the two independent spectra shown in Fig. 3(c), the solid curve belongs to the true target and the dotted one belongs to the false target. Clearly, one can now figure out which represents the true target after comparison with the spectrum of the transmitted chirp.

B) Countering jamming modes (b and c)

In this case, the jamming pulses are overlapped with the true target echo at the input of FrFT, and they have a narrower bandwidth than the true target echo. Figures 4(a) and 4(b) show the simulation results of the proposed anti-jamming technique when as an example there are eight jamming pulses. After FrFT pulse compression and filtering, each compressed pulse is returned from fractional to frequency domains as shown in Fig. 4(c), the solid curve belongs to the true target and the dotted ones belong to the false targets. Clearly, one can now figure out which represents the true target after comparison with the spectrum of the transmitted chirp.

VI. CONCLUSIVE REMARKS

We have shown that the proposed anti-jamming technique benefits from the pulse compression gain of FrFT and its capability to separate the overlapping chirps in time and frequency domains, which cannot be achieved using a standard matched filter. But this happens at a cost of 3 dB in terms of SNR. In addition, it was shown that using CFAR extensions, e.g. SOCA-CFAR, CS-CFAR, and OS-CFAR, this can not only overcame the mutual target masking problem due to high JSR, but also this introduces a higher CFAR loss above the conventional CFAR. To the best of the authors' knowledge, and apart from what is given by [16], other ECCM techniques cannot be used to counter jammers of the sort assumed in this paper.

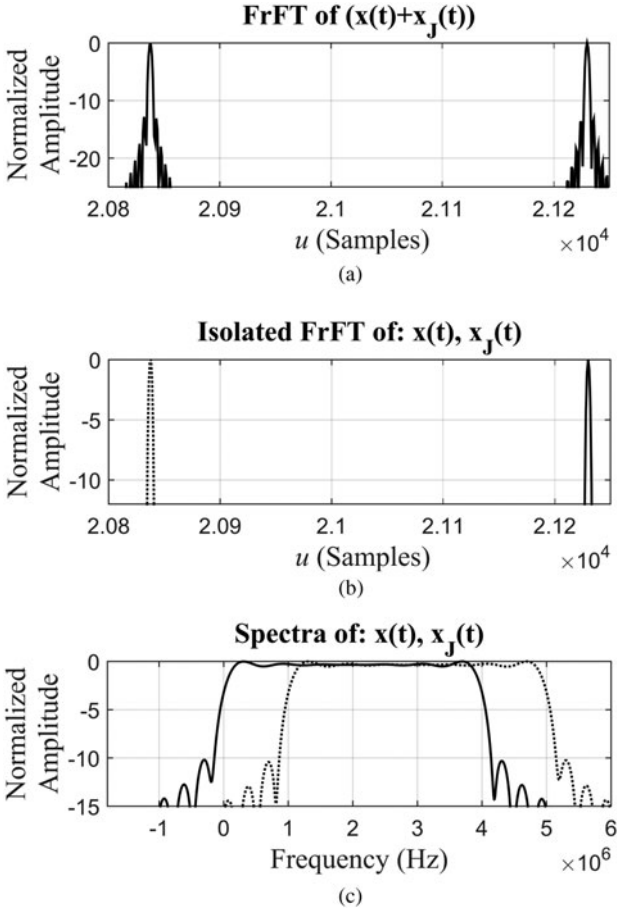

Fig. 3. Countering single false targets jamming. (a) The FrFT of the received signal. (b) The main lobes after separation. (c) The spectra of separated signals.

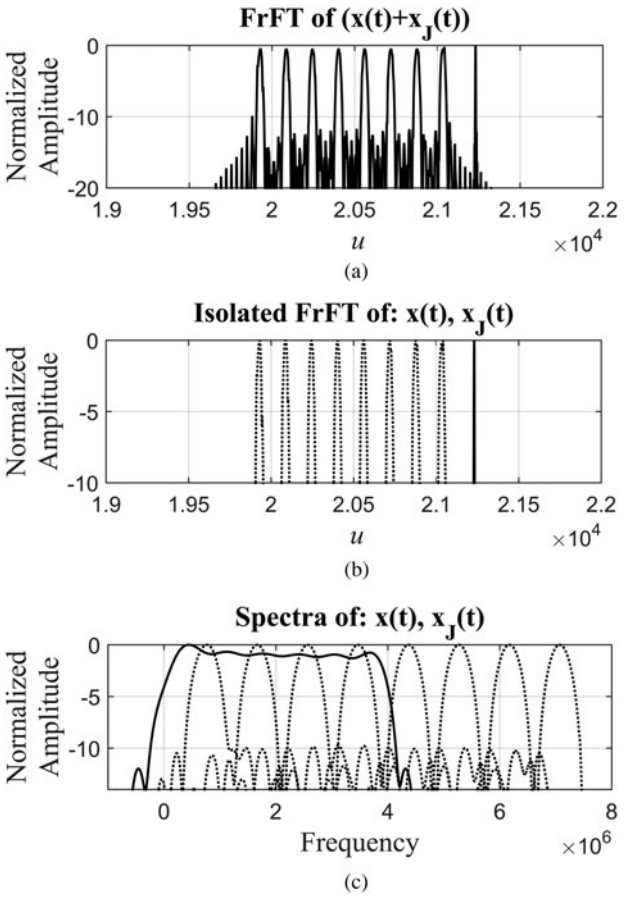

Fig. 4. Countering multiple-false targets jamming. (a) The FrFT of the received signal. (b) The main lobes after separation. (c) The spectra of separated signals.

https://doi.org/10.1017/S1759078717000289 Published online by Cambridge University Press

VII. CONCLUSION

The conflict between jamming and anti-jamming is a permanent combat. There is no jamming that cannot be suppressed, and no radar that cannot be jammed. In this paper, we proposed anti-jamming technique based on the FrFT to counter self-protection frequency-shifting jammer against surveillance chirp radar. The theoretical analysis and simulation results show that FrFT can compress and separate the overlapping true target echo and jamming signal, and then the true target is discriminated after the comparison between the spectrum of each separated signal and the spectrum of the transmitted chirp in term of the center frequency and sweep bandwidth. Despite the fact that the FrFT is inferior to the matched filter by 3 dB. The proposed technique works well where a matched filter does not work. In addition, it is suitable for practical application.

ACKNOWLEDGEMENT

The authors would like to thank Hatem Najdi for his helpful discussions and for reviewing the final version of this paper.

REFERENCES

[1] Curtis Schleher, D.: Electronic Warfare in the Information Age, chapter 4, Artech House, Boston–London, 1999.

[2] De Martino, A..: Introduction to Modern EW Systems, chapter 5, Copyright © 2012 by Artech House, Boston–London, 2012.

[3] Yong, Y.; Zhang, W.-M.; Yang, J.-H.: Study on frequency-shifting jamming to linear frequency modulation pulse compression radars, in Wireless Communications & Signal Processing, IEEE, 2009, 1–5.

[4] Sun, H.-B.; Liu, G.-S.; Gu, H.; Su, W.-M.: Application of the fractional Fourier transform to moving target detection in airborne SAR. IEEE Trans. Aerosp. Electron. Syst., **38** (4) (2002), 1416–1424.

[5] Cowell, D.M.J.; Freear, S.: Separation of overlapping linear frequency modulated (LFM) signals using the fractional Fourier transform. IEEE Trans. Ultrason. Ferroelectr. Freq. Control, **57** (10) (2010), 2324–2333.

[6] Elgamel, S.A.; Soraghan, J.J.: Radar matched filtering using the fractional Fourier transform, in Sensor Signal Processing for Defence (SSPD 2010), 29 September 2010, IET, 1–5.

[7] Akay, O.; Erzden, E.: Employing fractional autocorrelation for fast detection and sweep rate estimation of pulse compression radar waveforms. Signal Process., **89** (12) (2009), 2479–2489. (Special Section: Visual Information Analysis for Security).

[8] Elgamel, S.A.; Soraghan, J.J.: Enhanced monopulse radar tracking using filtering in fractional Fourier domain, in 2010 IEEE Radar Conf., IEEE, 10 May 2010, 247–250.

[9] Skolnik, M.: Radar Handbook, 3rd ed., chapter 24, McGraw-Hill, USA, 2008. ISBN: 978-0071485470.

[10] Adamy, D.L.: EW 104, EW against a New Generation of Threats, chapter 4. Copyright © 2015 by Artech House, Boston–London, 2015. ISBN 13: 978-1-60807-869-1.

[11] Deng, H.: Polyphase code design for orthogonal netted radar systems. IEEE Trans. Signal Process., **52** (11) (2004), 3126–3135.

[12] Elgamel, S.A.; Soraghan, J.J.: Fractional Fourier Transform based monopulse radar for combating jamming interference, in Sensor Signal Processing for Defence (SSPD 2010), IET, 29 September 2010, 1–5.

[13] Bing, W. et al.: Deceptive jamming suppression based on coherent cancelling in multistatic radar system, in 2016 IEEE Radar Conf. (RadarConf), IEEE, 2 May 2016, 1–5.

[14] Ahmed, A. et al.: Subarray-based FDA radar to counteract deceptive ECM signals. EURASIP J. Adv. Signal Process. **7** (2016), 104.

[15] Xu, J. et al.: Deceptive jamming suppression with frequency diverse MIMO radar. Signal Process., **113** (2015), 9–17.

[16] Hanbali, S.B.S.; Kastantin, R.: Countering a self-protection frequency shifting jamming against LFM pulse compression radars. Int. J. Electron. Telecommun., **63** (2) (2017).

[17] Ozaktas, H.; Zalevsky, Z.; Kutay, M.: The Fractional Fourier Transform: with Applications in Optics and Signal Processing, Wiley, Chichester, UK, 2001, 99–107.

[18] Ozaktas, H.; Arikan, O.; Kutay, M.; Bozdagt, G.: Digital computation of the fractional Fourier transform. IEEE Trans. Signal Process., **44** (9) (1996), 2141–2150.

[19] Capus, C.; Rzhanov, Y.; Linnett, L.: The analysis of multiple linear chirp signals, in Time-scale and Time-Frequency Analysis and Applications (Ref. No. 2000/019), IEE Seminar on 2000, IET, 4–1.

[20] Capus, C.; Brown, K.: Short-time fractional Fourier methods for the time-frequency representation of chirp signals. J. Acoust. Soc. Am., **113** (6) (2003), 3253–3263.

[21] Almeida, L.B.: The fractional Fourier transform and time–frequency representations. IEEE Trans. Signal Proc., **42** (11) (1994), 3084–3093.

[22] Ashok Narayanana, V.; Prabhub, K.M.M.: The fractional Fourier transform: theory, implementation and error analysis, Science direct, Microprocess. Microsys., **27** (2003), 511–521.

[23] Guoh, Y.; Guan, J.: Detection of moving target based on fractional Fourier transform in SAR clutter, in 2010 IEEE 10th Int. Conf. Signal Processing (ICSP), 24 October 2010, IEEE, 2003–2006.

[24] Liu, J.-C.; Liu, Z.; Wang, X.-S.; Xiao, S.-P.; Wang, G.-Y.: SNR analysis of LFM signal with Gaussian white noise in fractional Fourier transform domain. J. Electron. Inf. Technol., **29** (10) (2007), 2337–2340.

[25] Cooley, J.W.; Tukey, J.W.: An algorithm for the machine calculation of complex Fourier series. Math. Comput., **19** (90) (1965), 297–301.

[26] Richards, M.A.: Fundamentals of Radar Signal Processing, 2nd ed., chapter 4, 6. McGraw-Hill, 2014, ISBN: 978-0-07-179833-4.

[27] Richards, M.A.; Scheer, J.A.; Holm, W.A.: Principles of Modern Radar, vol. **I**: Basic Principles, chapter 16, Copyright ©2010 by SciTech Publishing, 2010.

Samer Baher Safa Hanbali received a B.Sc. degree in Electronic Engineering from Damascus University, Syria, in 2000, and an M.Sc. degree from FH Joanneum, Austria, in 2011. He is pursuing a Ph.D. degree, in the area of radar signal processing, at the Department of Communication Engineering in the Higher Institute of Applied Sciences and Technology, Damascus, Syria.

Radwan Kastantin received a B.Sc. degree in Electronic Engineering from Damascus University, Syria, in 1986, and a Ph.D. degree from ICP-INPG, France, in 1996. He is a Professor of Communication and Signal Processing at the Department of Communication Engineering in the Higher Institute of Applied Sciences and Technology, Damascus, Syria.

https://doi.org/10.1017/S1759078717000289 Published online by Cambridge University Press